

Microstructure and Physical Properties of Sn-Bi-Pb-Cd-Zn Rapidly Solidified Alloys

Eman Kashita¹, Salah. M. M. Salman^{1,2}

¹Qassim Univesity, Ministry of High Education, Kingdom of Saudi Arabia

²Physics Department, Faculty of Science, Helwan University, Ain-Helwan

ABSTRACT

Adding other elements to tin-bismuth eutectic alloy makes them priceless for other applications such as medical applications (shielding blocks for cancer treatment) and low temperature melting solder for safety devices like sprinkler. Microstructure, hardness, melting point, electrical and mechanical properties of Sn₄₂Bi₂₁Pb₃₀Cd₅Zn₂ and Sn₄₂Bi₃₀Pb₁₀Cd₁₅Zn₃ rapidly solidified alloys has been investigated. The results show that, the used alloys consists of rhombohedral bismuth phase, body centered tin phase, HCP cadmium phase and Pb₇Bi₃ intermetallic phase. Also electrical resistivity, hardness, melting point and elastic modulus values of Sn- Bi- Pb- Zn- Cd alloys are lower compared to Sn- Bi eutectic alloy. From our results, it can produce fusible alloy with superior properties for different industrial applications by changing their compositions.

Keywords: Microstructure, Vickers Hardness, Internal Friction, Elastic Moduli, Electrical Resistivity, Rapidly Solidified Alloys

I. INTRODUCTION

Fusible alloys are low melting temperature compositions containing bismuth, lead, tin, cadmium or indium. Bismuth addition to lead and other alloying elements make uniquely attractive combinations for low melting point alloy which are also suitable for fusible soldering and shielding blocks in mega-volt radiotherapy. Many researches were done to evaluate and discuss structure and physical properties of bismuth- lead/ bismuth-tin eutectic alloys, bismuth- lead- tin, bismuth- lead- tin-cadmium, tin- antimony and other fusible alloys with other elements additions [1-15]. The aim of the present study is to investigate structure, electrical, mechanical and thermal properties of Bi- Sn- Pb- Zn- Cd rapidly solidified alloys to produce fusible alloy for soldering microelectronics, computer and shielding blocks.

II. METHODS AND MATERIAL

Using high purity, more than 99.95%, tin, bismuth, lead, cadmium and zinc elements, the Bi- Sn- Pb- Zn- Cd

alloys were molten in the muffle furnace. To increase the homogeneity of the ingots the resulting ingots were turned and re-melted numerous times. From these ingots, long ribbons of about 3-5 mm width and ~ 80 μm thickness were prepared as the test samples by directing a stream of molten alloy onto the outer surface of rapidly revolving copper roller with surface velocity 31 m/s giving a cooling rate of 3.7×10^5 K/s. Using double knife cutter the samples then cut into convenient shape for the measurements. Structure of tin- antimony based alloys was performed using an Shimadzu x-ray diffractometer (Dx-30, Japan) of Cu-K α radiation with $\lambda=1.54056 \text{ \AA}$ at 45 kV and 35 mA and Ni-filter in the angular range 2θ ranging from 20 to 80° in continuous mode with a scan speed 5 deg/min. A digital Vickers micro-hardness tester, (Model-FM-7- Japan), was used to measure Vickers hardness values of used alloys. Internal friction Q^{-1} and the elastic constants of tin-antimony based alloys were determined using the dynamic resonance method [16- 18]. Electrical resistivity of used alloys was measured by a conventional double bridge method.

III. RESULTS AND DISCUSSION

A. Microstructure

X-ray diffraction patterns of $\text{Sn}_{42}\text{Bi}_{21}\text{Pb}_{30}\text{Cd}_5\text{Zn}_2$ and $\text{Sn}_{42}\text{Bi}_{30}\text{Pb}_{10}\text{Cd}_{15}\text{Zn}_3$ rapidly solidified alloys show that sharp lines of rhombohedral bismuth phase, body centered tin phase, HCP cadmium phase and Pb_7Bi_3 intermetallic phase as offered in Figure 1. X-ray analysis such as 2θ , d Å, intensity%, phase and hkl planes are presented in Table 1(a and b). From x-ray analysis, matrix microstructure and the shape of formed phases (peak intensity, peak broadness and peak position) of $\text{Sn}_{42}\text{Bi}_{21}\text{Pb}_{30}\text{Cd}_5\text{Zn}_2$ and $\text{Sn}_{42}\text{Bi}_{30}\text{Pb}_{10}\text{Cd}_{15}\text{Zn}_3$ alloys changed with changing alloys compositions. That is because some atoms dissolved in the tin- bismuth matrix formed a solid solution/or and some atoms formed a traces of undetected phases or intermetallic phases.

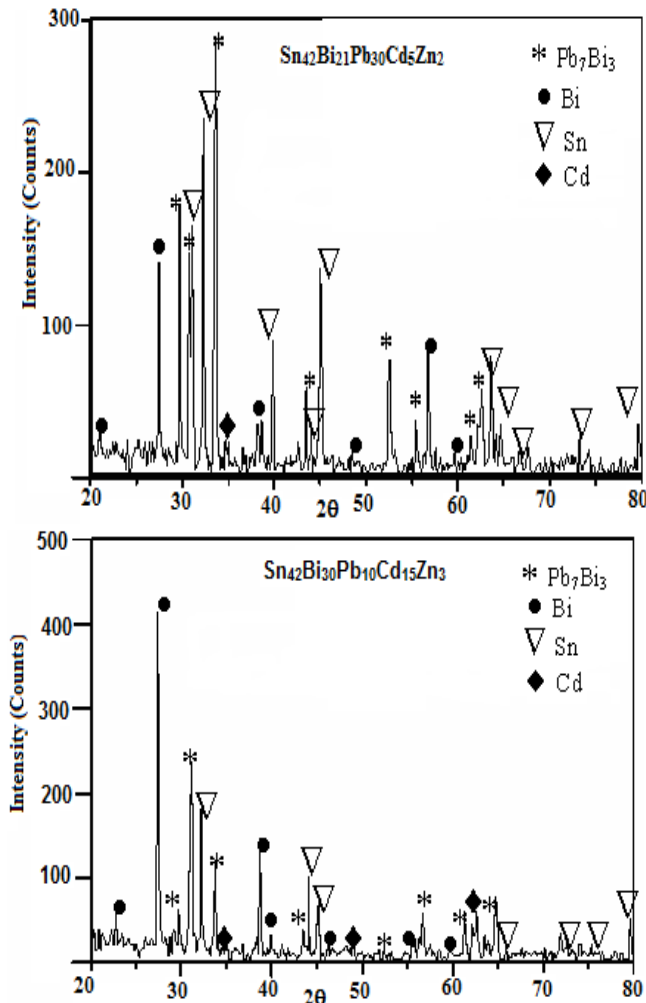


Figure 1: x-ray diffraction patterns of Bi- Sn- Pb- Zn- Cd alloys

Table (1a):- x-ray analysis of $\text{Sn}_{42}\text{Bi}_{21}\text{Pb}_{30}\text{Cd}_5\text{Zn}_2$ alloy

2θ	d Å	Int. %	phase	h k l
22.465	3.95453	6.4	Bi	003
27.187	3.27744	26.9	Bi	012
29.443	3.0312	40.2	Pb_7Bi_3	100
30.587	2.92042	50.7	Sn	200
30.865	2.8947	31.4	Pb_7Bi_3	002
31.984	2.79602	51.1	Sn	101
33.338	2.68546	100	Pb_7Bi_3	101
34.977	2.56327	1.9	Cd	002
37.959	2.36847	11.1	Bi	104
38.378	2.34357	7	Bi	104
39.668	2.27028	10.7	Bi	110
43.184	2.09323	15.7	Pb_7Bi_3	102
43.808	2.06484	11.6	Sn	220
44.843	2.01958	30.8	Sn	211
48.71	1.86789	1.9	Bi	202
52.23	1.75	26.2	Pb_7Bi_3	110
55.26	1.66098	11.2	Sn	301
56.043	1.63963	9	Bi	024
56.46	1.62849	24.8	Pb_7Bi_3	103
59.225	1.5589	3.5	Bi	107
61.121	1.51499	3.9	Sn	205
61.886	1.49811	15	Sn	116
62.372	1.48759	10.3	Sn	112
63.344	1.46708	16.1	Pb_7Bi_3	201
64.497	1.44361	10.7	Sn	321
72.222	1.30702	8.8	Sn	104
73.029	1.29457	8.6	Sn	411
79.364	1.20637	13.9	Sn	312
79.613	1.20322	8.4	Sn	312

Table (1b):- x-ray analysis of $\text{Sn}_{42}\text{Bi}_{30}\text{Pb}_{10}\text{Cd}_{15}\text{Zn}_3$ alloy

2θ	d Å	Int. %	phase	h k l
22.537	3.94196	4.2	Bi	003
27.26	3.26881	100	Bi	012
29.519	3.02361	8.7	Pb_7Bi_3	100
30.652	2.91436	25.9	Sn	200
30.938	2.88808	30.3	Pb_7Bi_3	002
32.045	2.79082	27.3	Sn	101
33.411	2.67971	21.6	Pb_7Bi_3	101
34.844	2.57276	1.7	Cd	100
38.016	2.36506	6.3	Bi	104
38.446	2.33957	11.2	Cd	101
39.719	2.2675	3.2	Bi	110
43.241	2.09061	3.7	Pb_7Bi_3	102
43.876	2.06183	6.6	Sn	220
44.905	2.01691	16.1	Sn	211
45.964	1.97289	2.7	Bi	006
48.02	1.8931	2.5	Cd	102
52.305	1.74766	3.1	Pb_7Bi_3	110
55.288	1.66021	4.1	Sn	301
56.137	1.6371	11	Bi	024
56.465	1.62836	4.9	Pb_7Bi_3	103
59.328	1.55644	3.2	Bi	107
61.177	1.51375	4	Cd	103
61.833	1.49926	3.9	Bi	116

62.119	1.49304	5.6	Cd	110
62.461	1.48568	6.5	Sn	112
63.679	1.46018	2	Pb ₇ Bi ₃	201
64.576	1.44203	2.1	Sn	122
72.353	1.30498	1.8	Sn	104
73.058	1.29412	3.7	Sn	411
79.391	1.20602	6.4	Sn	312

Scanning electron micrographs of Sn₄₂Bi₂₁Pb₃₀Cd₅Zn₂ and Sn₄₂Bi₃₀Pb₁₀Cd₁₅Zn₃ rapidly solidified alloys are shown in Figure 2. SEM of Sn₄₂Bi₂₁Pb₃₀Cd₅Zn₂ and Sn₄₂Bi₃₀Pb₁₀Cd₁₅Zn₃ alloys show needle structure of bismuth, structure of the intermetallic compound of Pb₇Bi₃ which like foot and clusters of the composed atoms.

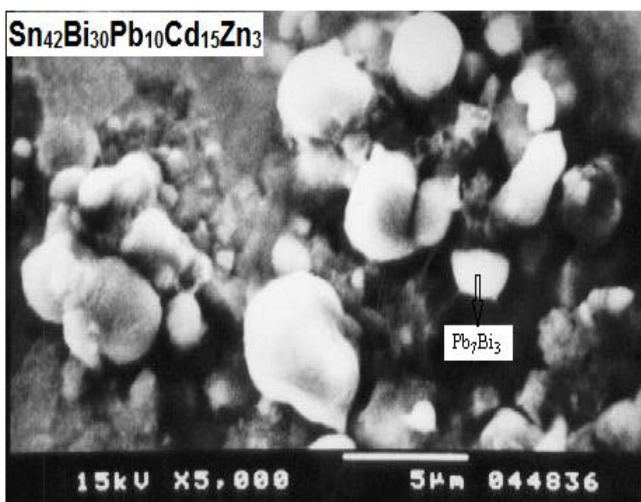
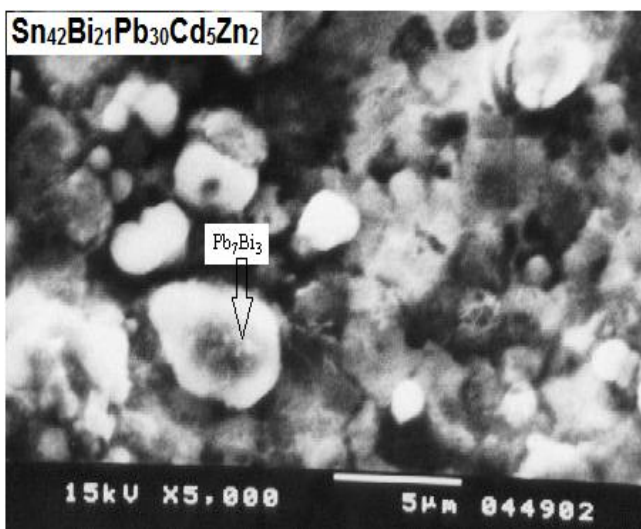


Figure 1: SEM of Bi- Sn- Pb- Zn- Cd alloys

B. Mechanical properties

Elastic moduli

The elastic constants are directly related to atomic bonding, structure and atomic density. The measured elastic modulus, E, and calculated shear modulus, μ , of Sn₄₂Bi₂₁Pb₃₀Cd₅Zn₂ and Sn₄₂Bi₃₀Pb₁₀Cd₁₅Zn₃ alloys are listed in Table 2. Elastic modulus value of tin-bismuth eutectic alloy decreased after adding different alloying elements which dependent on alloy composition as shown in Table 2. That is because the dissolved atoms formed solid solution\ or stick on grain boundary/ or formed a small cluster in matrix, changed bond matrix strengthens.

Internal friction

Internal friction is a useful tool for the study of structural features of alloys. Calculated internal friction values of Sn₄₂Bi₂₁Pb₃₀Cd₅Zn₂ and Sn₄₂Bi₃₀Pb₁₀Cd₁₅Zn₃ alloys are presented in Table 2. The results show that, internal friction value of used alloys are approximately the same and it's lower than the Bi- Sn eutectic alloy.

Vickers microhardness and minimum shear stress

The hardness is the property of material, which gives it the capability to resist being enduringly deformed when a load is applied. The better of material hardness is the highest of the resistance to deformation. The Vickers hardness of Sn₄₂Bi₂₁Pb₃₀Cd₅Zn₂ and Sn₄₂Bi₃₀Pb₁₀Cd₁₅Zn₃ alloys at 10 gram force and indentation time 5 sec are shown in Table 3. Also calculated minimum shear stress, μ_n , of Sn₄₂Bi₂₁Pb₃₀Cd₅Zn₂ and Sn₄₂Bi₃₀Pb₁₀Cd₁₅Zn₃ alloys are listed in Table 3. Vickers hardness value of tin-bismuth eutectic alloy is decreased after adding Pb, Cd and Zn with different ratio.

Table 2:- elastic modulus, internal friction and thermal diffusivity of Sn-Bi-Pb-Cd-Zn alloys

Alloys	E GPa	Q ⁻¹	μ GPa	μ/E
Bi ₅₈ Sn ₄₂	22.41 ± 0.9	0.048	8.354	0.373
Sn ₄₂ Bi ₃₀ Pb ₁₀ Cd ₁₅ Zn ₃	16.19 ± 1.4	0.011	6.017	0.372
Sn ₄₂ Bi ₂₁ Pb ₃₀ Cd ₅ Zn ₂	18.04 ± 1.9	0.011	6.577	0.365

Table 3:- Vickers hardness and minimum shear stress of Sn-Bi-Pb-Cd-Zn alloys

Alloys	H_v kg/mm ²	μ_n kg/mm ²
Bi ₅₈ Sn ₄₂	21.5 ± 0.66	7.095
Sn ₄₂ Bi ₃₀ Pb ₁₀ Cd ₁₅ Zn ₃	15.71 ± 0.5	5.18
Sn ₄₂ Bi ₂₁ Pb ₃₀ Cd ₅ Zn ₂	12.68 ± 1.2	4.18

C. Electrical resistivity

Plastic deformation and crystalline imperfections raised electrical resistivity as a result of increasing the number of electron scattering centers. The measured electrical resistivity of Sn₄₂Bi₂₁Pb₃₀Cd₅Zn₂ and Sn₄₂Bi₃₀Pb₁₀Cd₁₅Zn₃ alloys at room temperature are shown in Table 4. Electrical resistivity value of tin-bismuth eutectic alloy decreased after adding alloying elements (Pb, Cd and Zn). That is because some atoms dissolved in the tin- bismuth matrix formed a solid solution/or and some traces decreased scattering center for conduction electrons which decreased electrical resistivity value

Table 4:- electrical resistivity of resistivity of Sn-Bi-Pb-Cd-Zn alloys

Samples	$\rho \times 10^{-8} \Omega.m$
Bi ₅₈ Sn ₄₂	59.44 ± 1.164
Sn ₄₂ Bi ₃₀ Pb ₁₀ Cd ₁₅ Zn ₃	44.84 ± 1.59
Sn ₄₂ Bi ₂₁ Pb ₃₀ Cd ₅ Zn ₂	45.69 ± 1.42

IV. CONCLUSION

1. X-ray diffraction analysis show that, Zn and Pb dissolved in Sn-Bi matrix formed solid solution and Pb₇Bi₃ intermetallic compound which affected all measured physical properties.
2. Elastic modulus, Vickers hardness, internal friction and electrical resistivity values of tin-bismuth eutectic alloy decreased after adding different ratio from Pb, Cd and Zn.

V. REFERENCES

- [1] M. Kamal, S. Mazen, A. B. El- Bediwi, E. Kashita, Radia. Eff. Def. Sol. 161 (2006) 143- 148
- [2] A. B. El-Bediwi and M.M. El-Bahay, Radia. Eff. Def. Sol. 159 (2004) 133- 140
- [3] M. Kamal, A. B. El- Bediwi, Radia. Eff. Def. Sol. 159 (2004) 651
- [4] A. B. El- Bediwi, E. Gouda, M. Kamal, A. M. S. E. Modeling C, 65:1 (2004)
- [5] A. B. El-Bediwi, M.M. El-Bahay, M. Kamal, Radia. Eff. Def. Sol. 159 (2004) 491- 496
- [6] M. Kamal, M. B. Karman and A. B. El-Bediwi, U. Scientist Phyl. Sci. 9: 2 (1997) 164 - 171
- [7] M. Kamal, A. B. El-Bediwi and M. B. Karman, J. Mater. Sci.: Mater. Electro. 9 (1998) 425- 428
- [8] M. Kamal, A. B. El-Bediwi, J. Mater. Sci.: Mater. Electro. 11 (2000) 519-523
- [9] A. B. El-Bediwi, A. M. S. E. 75: 3 (2002) 1-12
- [10] M. Kamal, M. El-Tonsy, A. B. El- Bediwi, E. Kashita, phys. stat. sol. (a) 201: 9 (2004) 2029-2034
- [11] M. Kamal, A. B. El-Bediwi, T. El-Asharm, J. Mater. Sci. Mater. Electro. 15 (2004) 211-217
- [12] M. Kamal, M. S. Meikhail, A. B. El- Bediwi, E. Gouda, Radia. Eff. Def. Sol. 160 (2005) 37
- [13] A. B. El-Bediwi, F. Dawood, M. Kamal, J. Advanc. Phys. 7:3 (2015) 1952
- [14] A. B. El- Bediwi, F. Dawood, M. Kamal, Intern. J. Sci. Eng. Appl. 4:2 (2015) 60- 63
- [15] A. B. El- Bediwi, F. Dawood, M. Kamal, Intern. J. Curr. Res. 7: 5 (2015) 16433-16439
- [16] E. Schreiber, O. L. Anderson, and N. Soga, Elastic Constants and Their Measurements (McGraw-Hill, New York, pp. 82–125 (1973)
- [17] S. Timoshenko and J. N. Goddier, Theory of Elasticity, 2nd ed. (McGraw-Hill, New York, p. 277 (1951)
- [18] K. Nuttall, J. Inst. Met. 99, 266 (1971)